

Exciton condensation in thin film topological insulator

EUN GOOK MOON^{1,2}, CENKE XU²

¹ *Department of Physics, Harvard University, Cambridge MA 02138, USA*

² *Department of Physics, University of California, Santa Barbara, California 93106, USA*

PACS **nn.mm.xx** – First pacs description
PACS **nn.mm.xx** – Second pacs description
PACS **nn.mm.xx** – Third pacs description

Abstract – We study the many-body physics in thin film topological band insulator, where the inter-edge Coulomb interaction can lead to an exciton condensation transition. We investigate the universality class of the exciton condensation quantum critical point. With different chemical potentials and interactions, the exciton condensation can belong to $z = 2$ mean field, or 3d XY, or Yukawa-Higgs universality classes. The interplay between exciton condensate and the time-reversal symmetry breaking is also discussed. Predictions of our work can be tested experimentally by tuning the chemical potentials on both surfaces of the thin film through gate voltage. We also show that all the analysis of the exciton condensate can be directly applied to a spin-triplet superconductor phase with attractive inter-edge interaction.

Quantum phases protected by topology have shown enormous interesting behaviors. Despite of unusual quantized responses to external fields [1, 2], topological phases usually manifest themselves with their stable edge states. For instance, the three dimensional topological band insulator (TBI) is characterized by its single Dirac cone edge state, with the Dirac point located at the time-reversal (\mathcal{T}) invariant point in the edge Brillouin zone. These edge states were predicted theoretically, and also observed very successfully experimentally in materials such as BiSb, Bi₂Se₃ and Bi₂Te₃ [3–7, 9]. It was understood that \mathcal{T} is crucial to the stability of the edge states [7, 8, 10, 11], basically because one cannot open up a \mathcal{T} -invariant Dirac mass gap for a single edge. Enormous interests were devoted to the \mathcal{T} breaking at the edge states of TBI, including the cases with \mathcal{T} broken by magnetic impurities and broken spontaneously due to interactions [12–17].

In a thin film sample of TBI, since the two edges are close enough to interact with each other, \mathcal{T} is no longer sufficient to protect the stability of the edge states *i.e.* it is allowed to open up a \mathcal{T} invariant gap for both edge states. Recently, the gap at the edge states was indeed observed in experiments on thin film TBI, when the thickness of the film is small [18–20]. It was proposed that even without direct inter-edge tunnelling, the local Coulomb interaction can also gap out the edge states through exciton condensation [24] *i.e.* a particle-hole pair bound state across the thin film condenses. This effect is most prominent when a

specific biased gate voltage is applied to two edges, where there is a “nesting” between two Fermi surfaces, and the “exciton” susceptibility diverges [24]. Lately it was proposed that large dielectric constants of these materials increases the layer separation range over which the inter surface coherence survives [21]. In our current paper we hope to go beyond the mean-field consideration in Ref. [24] and study the critical properties of the exciton condensate physics.

We illustrate our main results of this paper in the phase diagram (Fig. 1) plotted against the chemical potentials of the two edges, which we assume can be separately tuned with gate voltages on both edges. The color in this phase diagram denotes the critical Coulomb interaction U_c required to drive the exciton condensate, and at the line $\mu_1 + \mu_2 = 0$ except for the origin, $U_c = 0$ due to the divergence of exciton susceptibility. In most area of this phase diagram, the quantum critical point (QCP) belongs to the $z = 2$ mean field universality class. At the origin $\mu_1 = \mu_2 = 0$, the transition is described by the Yukawa-Higgs theory; and at the special line $\mu_1 = \mu_2 \neq 0$, the transition belongs to the 3d XY universality class. The same phase diagram and universality classes apply to the superconducting transition with attractive inter-edge “Coulomb” interaction.

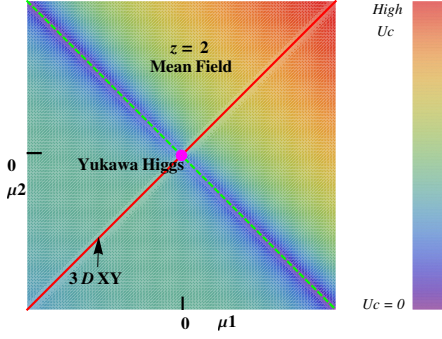


Fig. 1: The phase diagram of Eq. 1. The dark/bright colors denote the low/high critical Coulomb interaction.

The effective Hamiltonian of the surface states reads

$$\mathcal{H} = \sum_{l=1,2} \psi_l^\dagger (v_l \vec{\sigma} \cdot \vec{p} - \mu_l) \psi_l + U n_1 n_2, \quad (1)$$

where $v_l = (-1)^{l+1} v_f$ because the two edges of the TBI have opposite helicities. This Hamiltonian clearly has time-reversal symmetry $\mathcal{T} : \psi_l \rightarrow i\sigma^y \psi_l, \vec{k} \rightarrow -\vec{k}$. There is also an inversion symmetry $\mathcal{I} : \psi_1 \leftrightarrow \psi_2, \vec{k} \rightarrow -\vec{k}$ when $\mu_1 = \mu_2$, and the inversion is also a generic symmetry of materials such as Bi_2Te_3 and Bi_2Se_3 . Gate voltages determine the relative chemical potentials, μ_l . The second term of Eq. 1 describes the short ranged inter-edge Coulomb interaction. We assume the screening length of the thin film, therefore the inter-edge Coulomb interaction is still important even when the direct inter-edge electron tunnelling is ignorable. The intra-edge Coulomb interaction is also tentatively ignored in this Hamiltonian, its effects will be discussed later.

Without inter-edge tunnelling, electron number in each layer is independently conserved. This enlarged $U(1) \times U(1)$ symmetry is spontaneously broken down to the diagonal $U(1)$ symmetry by exciton condensation with order parameter $\phi \sim U \langle \psi_1^\dagger \psi_2 \rangle$, which also lowers the energy of the system. Then a mean field Hamiltonian can be obtained from the Hubbard-Stratonovich transformation of the original Hamiltonian Eq. 1 [24]:

$$H_{MF} = \sum_{l=1,2} \psi_l^\dagger (v_l \vec{\sigma} \cdot \vec{p} - \mu_l) \psi_l + (\phi^* \psi_1^\dagger \psi_2 + H.c.) + \frac{|\phi|^2}{U}.$$

The complex order parameter ϕ is invariant under \mathcal{T} , but becomes its complex conjugate under inversion \mathcal{I} . Clearly there are also other mean field channels of the Coulomb interaction such as $\langle \psi_1^\dagger \sigma^z \psi_2 \rangle$, but the exciton order $U \langle \psi_1^\dagger \psi_2 \rangle$ has the lowest mean field energy because it opens up a Dirac mass gap, therefore we will focus on this order parameter in our current work.

After integrating out the fermions, the static and uniform renormalization to the mean field Hamiltonian of ϕ

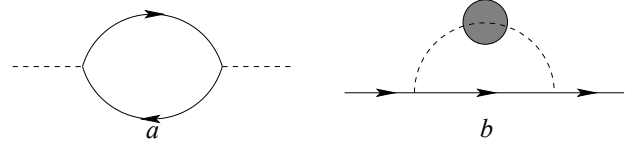


Fig. 2: *a*, one-loop Feynman diagram for renormalized Boson Lagrangian, *b*, Feynman diagram for the fermion self-energy. The dashed lines can denote either the exciton ϕ or exciton bilinear $|\phi|^2$. The solid line denotes the fermion propagator.

is $\mathcal{L}_{eff} = (\frac{1}{U} - \chi_0) |\phi|^2$, χ_0 is the susceptibility of order parameter ϕ which can be evaluated from Boson self-energy loop diagram Fig. 2:

$$\chi_0 = \Sigma_\phi(0,0) = - \int_{i\omega, k} \text{Tr}(\hat{G}_1(k, i\omega) \hat{G}_2(k, i\omega)), \quad (2)$$

where \hat{G}_l is Green's function of fermion. This integral increases linearly with the ultraviolet cut-off Λ *i.e.* it is not just a Fermi surface effect. For instance, when $\mu_1 = \mu_2 = \mu$, $\chi_0 \sim \Lambda - |\mu|$. Had we included the other mean field order parameter $\psi_1^\dagger \sigma^z \psi_2$, since the susceptibility of this order parameter only comes from the Fermi surface, it would never beat the order parameter $\phi \sim U \langle \psi_1^\dagger \psi_2 \rangle$ under consideration, as long as the size of the Fermi surface is small compared with the UV cut-off.

If we fix μ_2 , the critical Coulomb interaction U_c is plotted in Fig. 3. As we mentioned, U_c itself is cut-off dependent. However, the relative difference between U_c is UV cut-off independent, hence we can still compare U_c with no ambiguity. As we can see, at $\mu_1 = -\mu_2 \neq 0$, the critical Coulomb interaction is zero, due to the fact that the exciton susceptibility diverges logarithmically at this point. The logarithmic divergence is a consequence of the Fermi surface nesting between the two edges [24]. At $\mu_1 = \mu_2 \neq 0$, although the two Fermi surfaces still have the same size, the wavefunction overlap $\langle \psi_{1,\vec{k}} | \psi_{2,\vec{k}} \rangle = 0$ for any momentum \vec{k} at the Fermi surface, therefore the susceptibility is not divergent. This matrix element suppression is due to the opposite helicity of the two edges, and as we will see, this suppression will also affect the dynamics and universality class of QCP.

Now let us go beyond the mean field formalism and move on to the universality class of the QCPs. Without fermions, the exciton condensation would certainly belong to the 3d XY universality class, while coupling to Fermions will likely modify the universality class. Let us first discuss the case with $\mu_1 = \mu_2 = 0$. At this point, after redefining $\psi_2 \rightarrow \sigma_z \psi_2$, the phase transition is described by the following Lagrangian:

$$\begin{aligned} \mathcal{L}_{Higgs} &= \bar{\psi}_l \gamma^\mu \partial_\mu \psi_l + \lambda \vec{\phi} \cdot \vec{\psi} \bar{\eta} \psi \\ &+ |\partial_\tau \phi|^2 + v_\phi^2 |\nabla \phi|^2 + r |\phi|^2 + \frac{u}{4} |\phi|^4 + \dots \\ \vec{\eta} &= (\eta^x, \eta^y), \quad \vec{\phi} = (\text{Re}[\phi], \text{Im}[\phi]). \end{aligned}$$

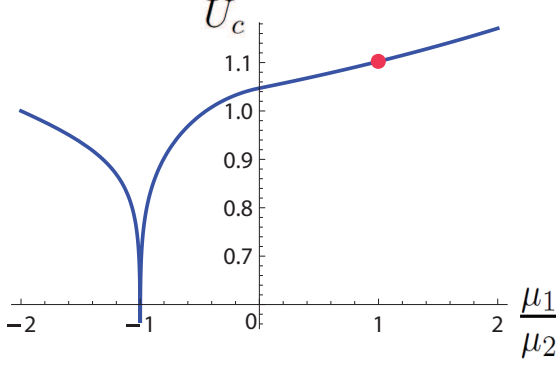


Fig. 3: The plot of critical Coulomb interaction U_c against chemical potential μ_1 , with fixed $\mu_2 > 0$. Critical Coulomb interaction is measured in units of the U_c with $\mu_1/\mu_2 = -2$. U_c is zero at $\mu_1 = -\mu_2$ due to the logarithmically divergent exciton susceptibility. Everywhere but $\mu_1 = \pm\mu_2$, the QCP have $z = 2$ dynamical exponents, with mean field universality class. The special point $\mu_1 = \mu_2 \neq 0$ (solid circle) has $z = 1$ dynamical scaling, and it belongs to the 3d XY universality class.

Here $\gamma_\mu = (\sigma^z, \sigma^x, \sigma^y)$, η^x and η^y are two Pauli matrices that mix the two edges. This model becomes precisely the Higgs-Yukawa model which describes the Chiral symmetry breaking of Dirac fermion, at least when $v_f = v_\phi$. The transition of $\vec{\phi}$ is not 3d XY transition because the coupling λ is relevant at the 3d XY fixed point, based on the well-known scaling dimensions $[\psi] = 1$, and $[\vec{\phi}] = (d-2)/2 + \eta/2 = 0.519$ at the 3d XY fixed point [22]. The critical exponents of this transition with large N have been calculated by means of $1/N$ and $\epsilon = 4 - d$ expansions [23, 25–27], and a second order transition with non-Wilson-Fisher universality class was found. Therefore we conclude that the transition is still second order, with different universality class from the 3d XY transition.

If $\mu_1 \neq \mu_2$, due to the mismatch of the size of the Fermi surface, the loop diagram Fig. 2 will not lead to singular behavior for Boson self-energy at low frequency and small momentum. However, the fermi surface mismatch breaks the inversion symmetry of the Hamiltonian Eq. 1, therefore the following term is allowed in the Lagrangian:

$$\mathcal{L}_1 = h(i\phi^x \partial_\tau \phi^y - i\phi^y \partial_\tau \phi^x) \sim h\phi^* \partial_\tau \phi, \quad h \sim \mu_2 - \mu_1. \quad (3)$$

\mathcal{L}_1 leads to a $z = 2$ dynamical exponent, which is analogous to the Mott insulator (MI) -superfluid transition in Bose Hubbard model away from the tip of MI lobe [28], and also the XY magnetic transition in magnetic field. In two spatial dimension, the $z = 2$ transition is a mean field transition with marginally irrelevant perturbations.

If $\mu_1 = \mu_2 \neq 0$, then the exciton condensation is similar to a ferromagnetic transition in Fermi liquid, which usually has $z = 3$ over damped quantum critical mode [29, 30]. However, in our case there is the matrix element

suppression effect mentioned before, namely:

$$\begin{aligned} |\mathcal{M}_{k,k+q}|^2 &= |\langle k+q, 1 | \psi_{1,k+q}^\dagger \psi_{2,k} | k, 2 \rangle|^2 \\ &= \sin^2(\theta_{k+q} - \theta_k) \sim q^2/k_f^2. \end{aligned} \quad (4)$$

This matrix element suppression strongly affects the low energy dynamics of the quantum critical fluctuations. For instance, the damping rate of the quantum critical modes due to particle-hole excitations can be calculated through the Boson self-energy diagram Fig. 2a:

$$\begin{aligned} \text{Im}[\Sigma_\phi(\omega, q)] &\sim g^2 \int \frac{d^2 k}{(2\pi)^2} [f(\epsilon_{k+q}) - f(\epsilon_k)] \\ &\times \delta(|\omega| - \epsilon_{k+q} + \epsilon_k) |\mathcal{M}_{k,k+q}|^2 \sim g^2 \frac{|\omega|q}{v_f k_f^2}. \end{aligned} \quad (5)$$

This term will not lead to over-damped $z = 3$ quantum critical modes. The same effect was noticed in Ref. [15] in the context of \mathcal{T} breaking at the edge state of TBI, and following the argument of Ref. [15], we can conclude that this transition still belongs to the 3d XY universality class even though the order parameter $\vec{\phi}$ couples linearly to Fermi surface in Eq. 2.

The quantum critical modes also modify the Fermion's self-energy. Using the Feynman diagram Fig. 2b, the Fermion self-energy reads

$$\Sigma(i\omega) \sim \int d^2 k d\epsilon G(i\epsilon + i\omega, \vec{k}) \langle \vec{\phi}_{i\epsilon, \vec{k}} \vec{\phi}_{-i\epsilon, -\vec{k}} \rangle |\mathcal{M}_{0,k}|^2 \quad (6)$$

Here we use the full correlation at the 3d XY fixed point: $\langle \vec{\phi}_{i\epsilon, \vec{k}} \vec{\phi}_{-i\epsilon, -\vec{k}} \rangle \sim (\epsilon^2 + v_\phi^2 k^2)^{-1+\eta/2}$, η is the anomalous dimension of the order parameter $\vec{\phi}$ at the 3d XY fixed point. The leading order contribution to the imaginary part of Fermion self-energy reads

$$\Sigma(\omega)'' \sim (\lambda)^2 |\omega|^{2+\eta} \text{sgn}[\omega] \ll |\omega|. \quad (7)$$

Therefore the Fermion self-energy correction is always dominated by the linear frequency term of the free electron propagator, the linear coupling λ does not destroy the Landau quasiparticles.

In addition to the linear coupling Eq. 2, another quadratic interaction is also allowed by symmetry, but was omitted in the mean field Hamiltonian Eq. 2:

$$\mathcal{L}' \sim \lambda' \sum_l \psi_l^\dagger \psi_l (\vec{\phi})^2. \quad (8)$$

When $\mu_1 = \mu_2 = 0$, this term is clearly irrelevant based on straightforward power-counting. With finite Fermi surfaces, after integrating out the fermions, this quadratic interaction will induce the following four-body interaction between $\vec{\phi}$:

$$\mathcal{L}_2 = u(\vec{\phi}_{i\omega, \vec{q}}^2 \frac{|\omega|}{q} (\vec{\phi}_{-i\omega, -\vec{q}}^2 + \dots \quad (9)$$

Note that the term with $|\omega|$ comes from the Fermi surface effects. We want to estimate the scaling dimension of u at the 3d XY fixed point. Since the scaling dimension $[(\vec{\phi})^2] = 3 - 1/\nu$, the scaling dimension of u is $[u] = 2/\nu - 3$, here ν is the standard critical exponent defined as $\xi \sim r^{-\nu}$. Therefore as long as $\nu > 2/3$, u is irrelevant. This criterion is indeed satisfied according to the well-known exponents of 3d $O(N)$ universality class [22]. \mathcal{L}_2 also exists at the $z = 2$ QCP with $\mu_1 \neq \mu_2$ discussed before, however, since there $[\omega] = 2[q] = 2$, this term has a high scaling dimension and is clearly irrelevant. A similar analysis about the $|\omega|/q$ term was first made in Ref. [31].

Again we can evaluate effect of the coupling \mathcal{L}' on the Fermion self-energy. The leading order correction can again be calculated through diagram Fig. 2b, while now the dashed lines are correlation functions $\langle \vec{\phi}_{i\epsilon, \vec{k}}^2 \vec{\phi}_{-i\epsilon, -\vec{k}}^2 \rangle \sim (\epsilon^2 + v_\phi^2 k^2)^{\frac{3}{2} - \frac{1}{\nu}}$. With finite Fermi surface, the leading order contribution to the imaginary part of fermion self-energy reads

$$\Sigma(\omega)'' \sim (\lambda')^2 |\omega|^{5-2/\nu} \text{sgn}[\omega] \ll |\omega|. \quad (10)$$

Hence this quadratic coupling \mathcal{L}' does not destroy the Landau quasiparticle at the QCP either.

Now let us turn on an extra intra-edge Coulomb interaction in Eq. 1:

$$\mathcal{L}_v = \sum_l V n_{l,\uparrow} n_{l,\downarrow} \quad (11)$$

This term will favor to develop magnetization on each edge [17]. Since $V n_{l,\uparrow} n_{l,\downarrow} \sim -V(\psi_l^\dagger \sigma^z \psi_l)^2/2$, the Hubbard-Stratonovich transformation can give us mean field order parameter $\Phi_1 \sim \langle \psi^\dagger \sigma^z \psi \rangle$ and $\Phi_2 \sim \langle \psi^\dagger \sigma^z \eta^z \psi \rangle$ with Ising symmetry. Without exciton condensate in the background, these two Ising order parameters Φ_1 and Φ_2 are degenerate at the mean field level. Φ_1 breaks only \mathcal{T} , while Φ_2 breaks both \mathcal{T} and \mathcal{I} . In the background of exciton condensate, Φ_2 has lower fermion mean field energy because the exciton order parameters anticommute with Φ_2 , hence the exciton condensate favors to have a \mathcal{I} breaking magnetization.

In Ref. [24], it was shown that when $\mu_1 + \mu_2 = 0$, at the vortex core of the exciton condensate order parameter there is a Fermion zero mode, which carries charge $\frac{1}{2}$. This zero mode is protected by the symmetry of Hamiltonian Eq. 1: $\gamma_2 H^* \gamma_2 = H$, and $\gamma_2 = i\sigma^y \eta^y$. This symmetry guarantees that the spectrum is symmetric with $E = 0$, and it is valid even with the presence of exciton vortex. With nonzero Φ_2 , this symmetry is broken, and there is no longer a zero mode at vortex core. By contrast, if the system develops magnetization Φ_1 , there is still a vortex core Fermion mode at precisely zero energy.

Just like the exciton order parameter ϕ , the order parameter Φ_a also couples to the Fermions both linearly and quadratically. Due to the same matrix element suppression effect as in Eq. 5, the linear coupling does not lead to singular corrections to the QCP of Φ_a . However, using

the similar argument as that below Eq. 9, the quadratic coupling $\mathcal{L}' \sim \lambda \sum_l \psi_l^\dagger \psi_l (\Phi_a)^2$ will lead to a relevant perturbation at the 3d Ising fixed point as long as one of the edges has a finite Fermi surface, due to the fact $\nu < 2/3$ at the 3d Ising universality class [22].

In addition to the Fermi surface, the Goldstone mode of the exciton condensate couples to order parameter Φ_a as well, if the QCP of Φ_a occurs in a background of exciton condensate. In the case without \mathcal{I} ($\mu_1 \neq \mu_2$), the lowest order coupling reads $\mathcal{L}'' \sim \lambda'' (\partial_\tau \theta) (\Phi_a)^2$. θ is the phase angle of the exciton condensate: $\phi \sim e^{i\theta}$. With \mathcal{L}'' , after integrating out the Goldstone mode θ , a singular term is induced for Φ_a :

$$\mathcal{L}_3 = u_3 (\Phi_a)_{i\omega, \vec{q}}^2 \frac{\omega^2}{\omega^2 + v_\phi^2 q^2} (\Phi_a)_{-i\omega, -\vec{q}}^2. \quad (12)$$

To determine the scaling dimension of this term, we again have to compare ν of 3d Ising transition and $2/3$: since $\nu < 2/3$, this coupling \mathcal{L}_3 is also relevant at the 3d Ising universality class. This relevant perturbation exists even when the Fermions are fully gapped out by the exciton condensate. In the case with \mathcal{I} , the coupling \mathcal{L}'' is forbidden, since $\theta \rightarrow -\theta$ under \mathcal{I} . In this case the coupling between Φ_a and the exciton Goldstone mode will occur at higher order, hence no relevant perturbation is induced at the 3d Ising universality class.

Although the exciton is charge neutral, its transport effect has been verified in bilayer quantum Hall system [35], by measuring the tunnelling conductance between the two layers [34]. A similar measurement can in principle be carried out in the thin film topological insulator. The exciton condensate will lead to a sharp peak of the inter-surface tunnelling conductance. Inside the exciton condensate phase, the condensate will be destroyed by the thermal fluctuation through a Kosterlitz-Thouless transition at finite temperature. The scaling between the critical temperature T_c of this KT transition and the tuning parameter r depends on the universality class of the QCP, and r can be taken as the interaction $U - U_c$. For example, for the $z = 2$ mean field transition, $T_c \sim |r|$; while for the 3D XY transition in the phase diagram (Fig. 1), $T_c \sim |r|^{z\nu} \sim |r|^{2/3}$. Thus different quantum critical behaviors can be measured through T_c . The interaction U between the two surfaces can be tuned by changing the thickness of the thin film sample.

If U in Eq. 1 is attractive instead of repulsive, then the system favors to have superconductor pairing. After a particle-hole transformation for ψ_2 : $\psi_2 \rightarrow \sigma^x \psi_2^\dagger$, both U and μ_2 change sign, while all the other terms of the Hamiltonian remain unchanged. The most energetically favored pairing state is $\psi_1 \sigma^x \psi_2$, because after particle-hole transformation this pairing becomes the exciton condensate ϕ . Therefore all the analysis of the QCP and Goldstone mode about this superconducting state can be obtained by particle-hole transformation of the exciton case. For instance, at chemical potential $\mu_1 = \mu_2$, there

is a logarithmic divergence of pairing susceptibility, while at $\mu_1 = -\mu_2$ there is a matrix element suppression at the interaction vertex between Cooper pair and fermions. The pairing $\psi_1 \sigma^x \psi_2$ is a spin triplet pairing with total $S^z = 0$, and the vortex core of this superconductor carries a fermion zero mode when $\mu_1 = \mu_2$.

In summary, we have studied the exciton condensation phase transition and its quantum critical properties in a phase diagram with edge dependent chemical potentials and Coulomb interaction. Interplay between exciton condensate and other order parameters are also discussed. In addition to the TBI materials that are currently under intensive experimental studies, we expect our formalism to be applicable to TBI with strong correlation, for instance the materials with 5d electrons [32, 33] which have been proposed recently.

* * *

The authors appreciate the very helpful discussions with Subir Sachdev. Eun Gook Moon is sponsored by the National Science Foundation under grant DMR-0757145, and also supported by the Samsung Scholarship.

REFERENCES

- [1] Xiao-Liang Qi, Taylor L. Hughes, Shou-Cheng Zhang 2008 *Phys. Rev. B* **78** 195424
- [2] Andrew M. Essin and Joel E. Moore and David Vanderbilt 2009 *Phys. Rev. Lett.* **102** 146805
- [3] Y. Xia, D. Qian, D. Hsieh, L. Wray, A. Pal, H. Lin, A. Bansil, D. Grauer, Y. S. Hor, R. J. Cava, M. Z. Hasan 2009 *Nature* **5** 398
- [4] D. Hsieh, Y. Xia, D. Qian, L. Wray, J. H. Dil, F. Meier, J. Osterwalder, L. Patthey, J. G. Checkelsky, N. P. Ong, A. V. Fedorov, H. Lin, A. Bansil, D. Grauer, Y. S. Hor, R. J. Cava, M. Z. Hasan 2009 *Nature* **460** 1101
- [5] Haijun Zhang, Chao-Xing Liu, Xiao-Liang Qi, Xi Dai, Zhong Fang, Shou-Cheng Zhang 2009 *Nature Physics* **5** 438
- [6] Y. L. Chen, J. G. Analytis, J. H. Chu, Z. K. Liu, S. K. Mo, X. L. Qi, H. J. Zhang, D. H. Lu, X. Dai, Z. Fang, S. C. Zhang, I. R. Fisher, Z. Hussain, Z. X. Shen 2009 *Science* **325** 178
- [7] Liang Fu, C. L. Kane, E. J. Mele 2007 *Phys. Rev. Lett.* **98** 106803
- [8] Liang Fu, C. L. Kane 2007 *Phys. Rev. B* **76** 045302
- [9] Liang Fu, C. L. Kane 2010 *Phys. Rev. Lett.* **100** 096407
- [10] C. L. Kane, E. J. Mele 2005 *Phys. Rev. Lett.* **95** 226801
- [11] C. L. Kane, E. J. Mele 2005 *Phys. Rev. Lett.* **95** 146802
- [12] Cenke Xu, Joel E. Moore 2006 *Phys. Rev. B* **73** 045322
- [13] Congjun Wu, B. Andrei Bernevig, Shou-Cheng Zhang 2006 *Phys. Rev. Lett.* **96** 106401
- [14] Qin Liu, Chao-Xing Liu, Cenke Xu, Xiao-Liang Qi, Shou-Cheng Zhang 2009 *Phys. Rev. Lett.* **102** 156603
- [15] Cenke Xu 2010 *Phys. Rev. B* **81** 020411
- [16] Cenke Xu 2010 *Phys. Rev. B* **81** 054403
- [17] Ying Ran, Hong Yao, Ashvin Vishwanath 2010 *Preprint arXiv:1003.0901*
- [18] Yao-Yi Li, Guang Wang, Xie-Gang Zhu, Min-Hao Liu, Cun Ye, Xi Chen, Ya-Yu Wang, Ke He, Li-Li Wang, Xu-Cun Ma, Hai-Jun Zhang, Xi Dai, Zhong Fang, Xin-Cheng Xie, Ying Liu, Xiao-Liang Qi, Jin-Feng Jia, Shou-Cheng Zhang, Qi-Kun Xue 2010 *Advanced Material* **22** 4002
- [19] Can-Li Song, Yi-Lin Wang, Ye-Ping Jiang, Yi Zhang, Cui-Zu Chang, Lili Wang, Ke He, Xi Chen, Jin-Feng Jia, Yayu Wang, Zhong Fang, Xi Dai, Xin-Cheng Xie, Xiao-Liang Qi, Shou-Cheng Zhang, Qi-Kun Xue, Xucun Ma 2010 *App. Phys. Lett.* **97** 143118
- [20] Sungjae Cho, Nicholas P. Butch, Johnpierre Palione, and Michael S. Fuhrer 2011, *Nano Letter* **11**, 1925
- [21] Dagim Tilahun, Byounghak Lee, E. M. Hankiewicz, and A. H. MacDonald 2010 *Phys. Rev. Lett.* **107** 246401
- [22] Pasquale Calabrese, Andrea Pelissetto, Ettore Vicari 2003 *Preprint cond-mat/0306273*
- [23] J. Zinn-Zustin 1991 *Nuc. Phys. B* **367** 105
- [24] B. Seradjeh, J. E. Moore, M. Franz 2009 *Phys. Rev. Lett.* **103** 066402
- [25] L. Karkkainen, R. Lacaze, P. Lacock, B. Petersson 1994 *Nuc. Phys. B* **415** 781
- [26] J. A. Gracey 1991 *Int. J. Mod. Phys. A* **6** 395
- [27] J. A. Gracey 1992 *Phys. Lett. B* **297** 293
- [28] Matthew P. A. Fisher, Peter B. Weichman, G. Grinstein, Daniel S. Fisher 1989 *Phys. Rev. B* **40** 546
- [29] J. A. Hertz 1976 *Phys. Rev. B* **14** 1165
- [30] A. J. Millis 1993 *Phys. Rev. B* **48** 7183
- [31] Subir Sachdev, T. Morinari 2002 *Phys. Rev. B* **66** 235117
- [32] A. Pesin, Leon Balents 2010 *Nature Physics* **6** 376
- [33] Atsuo Shitade, Hosho Katsura, Jan Kunes, Xiao-Liang Qi, Shou-Cheng Zhang, Naoto Nagaosa 2009 *Phys. Rev. Lett.* **102** 256403
- [34] Jung-Jung Su, A. H. MacDonald, *Nature Physics* **4**, 799
- [35] I. B. Spielman, J. P. Eisenstein, L. N. Pfeiffer, and K. W. West, *Phys. Rev. Lett.* **84**, 5808